Preprint
UCRL-JRNL-201372

Development of phosphor scintillator-based detectors for soft x-ray and vacuum ultraviolet spectroscopy of magnetically confined fusion plasmas

V.A.Soukhanovskii, S.P.Regan, M.J.May, M.Finkenthal, and H.W. Moos

U.S. Department of Energy
Lawrence Livermore National Laboratory

This article was submitted to Review of Scientific Instruments

December 10, 2003

DISCLAIMER

This work was performed under the auspices of the U.S. Department of Energy by the University of California, Lawrence Livermore National Laboratory under Contract No. W-7405-Eng-48.

Development of phosphor scintillator-based detectors for soft x-ray and vacuum ultraviolet spectroscopy of magnetically confined fusion plasmas

V. A. Soukhanovskii,[a] S. P. Regan,[b] M. J. May,[c] M. Finkenthal,[d] and H. W. Moos
Plasma Spectroscopy Group, Department of Physics and Astronomy, The Johns Hopkins University, Baltimore, Maryland 21218

Specialized soft x-ray and vacuum ultraviolet (VUV) diagnostics used to monitor impurity emissions from fusion plasmas are often placed in a very challenging experimental environment. Detectors in these diagnostics must be simple; mechanically robust; immune to electromagnetic interference, energetic particles, and magnetic fields up to several tesla; ultra-high-vacuum compatible; and able to withstand bakeout temperatures up to 300 °C. The design and the photometric calibration of a detector consisting of a P45 phosphor (Y_2O_2S:Tb), two incoherent fiber-optic bundles coupled with a vacuum feedthrough fiber-optic faceplate, and a photomultiplier tube (PMT) are reported. We have successfully operated the detectors of this type in novel soft x-ray and VUV diagnostics on several fusion plasma facilities. Measurements of the visible photon throughput of the silica/silica incoherent fiber-optic bundle, and the light loss associated with the coupling of the two fibers with the faceplate are presented. In addition, improved absolute measurements of the conversion efficiency of the P45/PMT photodetector based upon the use of a PMT with a bialkali photocathode instead of a multialkali one are presented for the soft x-ray and VUV range of photon wavelengths. The conversion efficiency is defined as the ratio of the photoelectrons ejected from the photocathode of a visible detector, which are excited by the scintillated photons that are emitted from the phosphor in a solid angle of 2π, to the number of soft x-ray photons incident on the phosphor. Sensitive electronic gain measurements of the PMT using the visible scintillated light from the P45 phosphor are compared with the gain measurements supplied by the manufacturer of the PMT, which were performed with a tungsten filament lamp operated at 2856 K.

I. INTRODUCTION

A detector comprising a phosphor scintillator acting as a wavelength shifter and a visible light detector, such as a photomultiplier tube (PMT), is commonly used in x-ray, soft x-ray, and vacuum ultraviolet (VUV) spectroscopy of high-temperature plasma.[1,2] In this article, we describe the detectors developed by our group for soft x-ray and VUV diagnostics used to monitor impurity emission in magnetically confined fusion plasma devices (tokamaks).[3–7] The instruments, typically, operate in very harsh environments, sometimes in close proximity to the plasmas. An example of an instrument with a phosphor/PMT detector is shown in Fig. 1.[5] A shoebox footprint extreme ultraviolet (XUV) monochromator was developed for monitoring the *NV* emission at 162 Å originating from the Alcator C-Mod tokamak divertor region. Improved plasma confinement, reduction of core impurity content, and reduction of thermal load on divertor plasma facing components were achieved in radiative divertor experiments with nitrogen injections in the Alcator C-Mod tokamak divertor.[8]

In this article, we discuss a design of the detector and present efficiency measurements of its components: an inorganic phosphor scintillator, a visible light extraction line, and a PMT. The requirements to the detectors are very stringent: they must be mechanically robust, and immune to electromagnetic fields, energetic particles, and high-energy photons. If some parts of the detector system share tokamak vacuum, they must be ultra-high-vacuum (UHV) compatible and be able to withstand bakeout temperatures 150–300 °C. Detector merits are determined by its temporal responsivity and its conversion efficiency (CE). The former is determined by the phosphor intrinsic properties, namely, the fluorescence and afterglow times. The detector conversion efficiency is defined as the ratio of the number of photoelectrons produced by a PMT photocathode to the number of soft x-ray or VUV photons incident on the phosphor. To understand and optimize the detector performance, several quantities must be measured independently and accurately, namely, the phosphor conversion efficiency, the PMT efficiency in the spectral range of phosphor emission, the electronic gain of the PMT, and the relay incoherent fiber-optic bundle losses. In

[a]Present address: Princeton Plasma Physics Laboratory, Princeton, NJ; electronic mail: vlad@pppl.gov
[b]Present address: Laboratory for Laser Energetics, University of Rochester, Rochester, NY.
[c]Present address: Lawrence Livermore National Laboratory, Livermore, CA.
[d]Permanent address: Racah Institute of Physics, Hebrew University, Jerusalem, Israel.

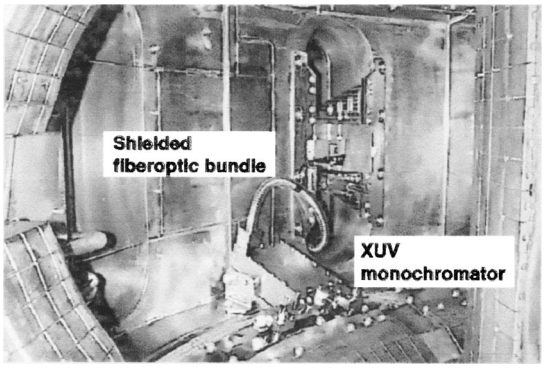

FIG. 1. Extreme ultraviolet multilayer mirror monochromator mounted on the divertor shelf of the Alcator C-Mod tokamak at MIT Plasma Science and Fusion Center.

our previous work, the conversion efficiency of several organic and inorganic phosphors were reported.[9,10] The P45 (Y_2O_2S:Tb) phosphor and a PMT with a multialkali photocathode was found to be an efficient detector in the range between 5 and 200 Å. In this article, we report the improved P45/bialkali PMT conversion efficiency measurements for soft x-ray and XUV photons, and, for the first time, for emission in the range between 300 and 2500 Å.

II. DETECTOR DESIGN

Three configurations of the phosphor/PMT and the optical couplings between them are examined in this article. Shown in Fig. 2(a) is a conceptual drawing of the XUV and VUV detectors used in the instruments described in Refs. 4, 6, and 7, respectively. This setup is defined hereafter as C1. The head-on PMT is located in the atmosphere and the phosphor is mounted on a glass window in the vacuum. The XUV version of this detector contains ultraviolet (UV) and visible light blocking metal foil filters with the bandpass window tailored for the XUV spectral region of interest. The VUV detector is used for monochromatic emission measurements and does not have foil filters. The utilization of the fiber optic link between the phosphor and the PMT is shown in Fig. 2(b) for the configuration defined as C2, with all components in the vacuum. Small F-number relay optics are not used to couple the visible light into the fiber-optic bundle, since they cannot be integrated with the compact design of our diagnostics due to mechanical constraints. In the event that the PMT is located in the atmosphere as shown in Fig. 2(c), a vacuum window consisting of a fused coherent fiber-optic faceplate provides the optical coupling of the vacuum side fiber with the atmosphere side fiber. This configuration is defined as C3. It has been used in the XUV monochromator shown in Fig. 1. The incoherent fiber optic bundles used are 3 m long and have circular cross sections (diameter $d=4.83$ mm). Each bundle consists of 331 individual fibers having a silica core (diameter $d=200\,\mu$m), a silica cladding ($200\,\mu\text{m}<d<210\,\mu$m), and a polyimide coating ($210\,\mu\text{m}<d<230\,\mu$m), and is encased in a Teflon [polytetrafluoroethylene (PTFE)] convolex with stainless steel ferrules on each end. The numerical aperture (NA) of the silica/silica fiber is 0.22. The total silica core area of all the 331 fibers comprises 57% of the cross-sectional area of the fiber bundle. The fiber-optic bundles were produced by Meteor Optics, Inc. Two types of PMTs were used in this study: a Hamamatsu model R1213 with a bialkali photocathode, and a Hamamatsu model R1464 with a multialkali photocathode. The beryllium 2200-Å-thick foil filter and the aluminum 1000-Å-thick foil filter have a measured visible transmission of 4×10^{-9}.[5] The P45 (Y_2O_2S:Tb) phosphor used in this work is manufactured by Thomson Electronics, Inc. The surface density is 1.5 mg/cm^2 and it was deposited on a glass substrate by the sedimentation method.

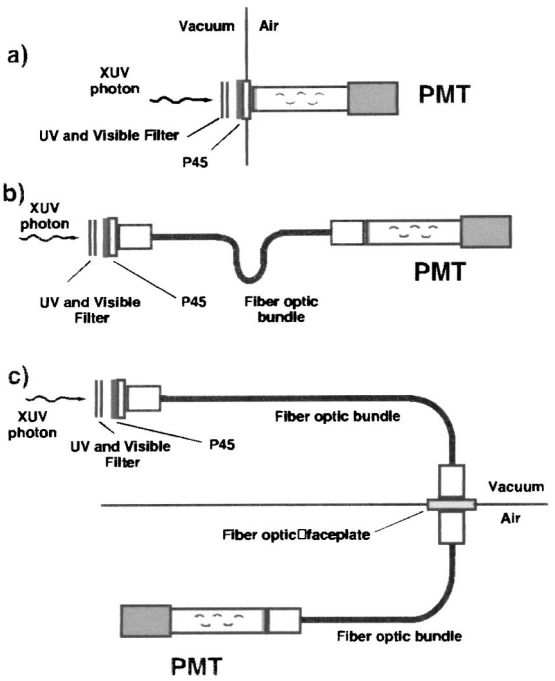

FIG. 2. Three configurations of the phosphor based detector: (a) phosphor/PMT (defined as C1), (b) phosphor/incoherent fiber optic bundle/PMT (defined as C2), and (c) phosphor/incoherent fiber-optic bundle/fused fiber-optic faceplate/incoherent fiber-optic bundle/PMT (defined as C3).

III. DETECTOR EFFICIENCY MEASUREMENTS

The CE measurements reported in this article were performed using the experimental technique outlined in Ref. 10. The accuracy of the measurement depends upon the accuracy of the PMT electronic gain measurement and the absolute photometric calibration of the reference detector. A gas flow proportional counter (GFPC) with a VYNS window was used as the reference detector for the measurements in the XUV range. It was operated with P-50 gas (50% argon/50% methane) for the 8.34, 9.89, 23.6, and 44.7 Å calibrations, and with propane for the 160 Å calibration. The GFPC efficiency was calculated using the measured transmissions of the VYNS window and gas absorption coefficients using Henke's low-energy x-ray interaction coefficients.[11] The data are summarized in Table I. The setup for the VUV measurements included a light source, a double monochromator, an absolutely calibrated detector, and the P45/PMT combination. A Penning reflex discharge operated with helium and argon buffer gases and carbon, aluminum, and copper cathodes, was used as a line radiation source in the range of

TABLE I. Gas flow proportional counter parameters.

Wavelength Å	Gas	Calculated absorption of gas	Measured transmission of VYNS window	Efficiency of XUV reference detector
8.34	P50	0.45	0.58	0.26
9.89	P50	0.62	0.57	0.35
23.6	P50	1.00	0.38	0.38
44.7	P50	1.00	0.27	0.27
160	Propane	1.00	0.127	0.127

100–2500 Å. A double monochromator used to isolate the wavelength of interest comprised two 0.25 m Minuteman 302 monochromators connected in series. A National Institute of Standards and Technology standard transfer detector (silicon photodiode) was used for absolute VUV photon measurements.

The electronic gain is defined as a ratio of the number of photoelectrons flowing from the photocathode to the number of electrons flowing through the anode of the PMT. Both the photocathode and the anode currents are measured. A Keithley Model 428 high gain current amplifier was used for the sensitive photocurrent measurements. A controlled solid angle geometrical factor was introduced during the anode current measurement in order to remain in the linear gain regime. The P45 phosphor irradiated with either $\lambda=9.89$ Å or $\lambda=44.7$ Å monochromatic light was used as a source of visible emission. A Hamamatsu E974-13 D-type socket was used as the voltage divider for the anode measurements; and a voltage of -1500 V (-1000 V) was applied across the divider of the bialkali (multialkali) PMT. In order to collect the photoelectrons ejected from the photocathode a voltage of -200 V (-135 V) was applied between the photocathode and the first dynode stage for the bialkali (multialkali) PMT. A comparison of our PMT gain measurements with those of the manufacturer is presented in Fig. 3. The Hamamatsu company measured the PMT gain using a tungsten filament lamp operated at 2856 K. The majority of our PMT gain measurements lie within the region enclosed by the two dashed lines, within 25% with the measurement of Hamamatsu.

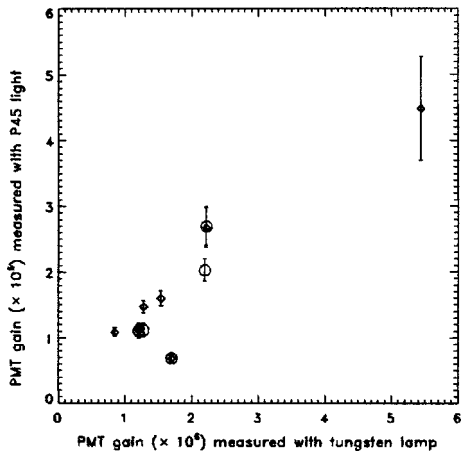

FIG. 3. Measured electronic gain of PMT using visible light from the P45 phosphor vs the gain measured by Hamamatsu using a tungsten lamp. Measurements made with carbon $K\alpha$ emission at 44.7 Å are represented by circles, and magnesium $K\alpha$ at 9.89 Å with diamonds. Dashed lines indicate $\pm 25\%$ deviation.

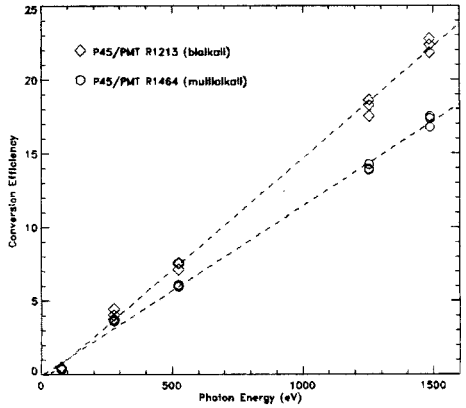

FIG. 4. Conversion efficiencies of the P45/PMT combination for a multialkali and a bialkali photocathode in the soft x-ray and XUV ranges.

Shown in Fig. 4 are the CE measurements obtained in the C1 configuration with a bialkali and a multialkali PMTs. The relevant experimental data is listed in Table II. The use of a PMT with a bialkali photocathode instead of a multialkali one increases the CE by a factor of 1.25.

Sodium salicilate and *P*-terphenyl are traditionally used in VUV phosphor-based detectors.[1] However, the properties of organic phosphors are incompatible with the UHV requirements of the magnetically confined fusion plasma facilities and inorganic phosphors remain the only alternative. CE measurements in the VUV range have been performed for the P45 phosphor and a PMT with a bialkali photocathode. Each point in Fig. 5 is an average of three to five measurements of the CE at various reflex discharge light intensities obtained by varying the discharge current. The VUV CE values are normalized to 4π (cf. 2π, as previously defined). The VUV flux densities incident on the reference detector were on the order of 10^7 photons/s. The P45/PMT conversion efficiency is variable across the VUV range, with a local peak at 1550 Å and several absorption edges around 2000 Å.

A. Efficiency of fiber-optic signal extraction line

The sensitivity of the detector is dependent on the losses in the optical relay channel between the phosphor and PMT and the quantum efficiency (QE) of the PMT's photocathode to the scintillated visible photons. In the forward 2π direc-

TABLE II. Measured parameters of PMT/P45 experiment.

Wavelength Å	PMT photocathode material	XUV photons/s incident on P45 phosphor	PMT photocurrent (nA)	Measured conversion efficiency
8.34	Bialkali	1.56×10^4	27.2	22.3
9.89	Bialkali	8.40×10^3	12.0	18.1
23.6	Bialkali	1.73×10^3	1.01	7.4
44.7	Bialkali	4.04×10^3	1.31	4.1
160	Bialkali	1.16×10^5	4.36	0.45
8.34	Multialkali	1.55×10^4	13.0	17.2
9.89	Multialkali	8.60×10^3	5.81	14.0
23.6	Multialkali	1.86×10^3	0.54	6.0
44.7	Multialkali	3.32×10^3	0.59	3.6
160	Multialkali	1.03×10^5	1.78	0.36

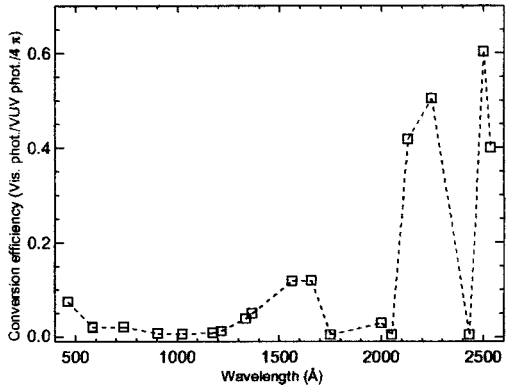

FIG. 5. Conversion efficiencies of the P45-multialkali PMT in the VUV range.

tion, the PMT in C1 collects 45% of the scintillated visible photons from the phosphor. In C2 and C3, the amount of visible scintillated light collected by the incoherent fiber-optic bundle is dependent on the NA of the silica/silica fiber, and the distance between the fiber-optic bundle and the phosphor. Aside from the photocathode efficiency, the signal measured by the PMT in C2 relies solely on the visible photon throughput of the fiber-optic bundle; however, the signal measured by C3 also depends upon the efficiency of the optical coupling between the vacuum fiber-optic bundle and the atmosphere fiber-optic bundle at the fused fiber-optic faceplate. Flux calculations of visible scintillated photons emitted by the phosphor and collected by detector configurations C1 and C2 were performed. The estimated signal of C2 relied on the use of a ray tracing code. The estimated signals of C1 and C2 were compared in order to evaluate the impact that the fiber-optic coupling has on the detector performance. The ratio of the estimated signals (C1 signal/C2 signal) is presented in Fig. 6 as a function of the radius of the XUV beam incident on the phosphor. A numerical aperture of 0.22 was assumed in the calculations presented in Fig. 6(a), and the distance between the phosphor and fiber-optic bundle was varied from 0.10 to 0.43 to 3.18 mm. The value of 0.10 mm corresponds to the case where the phosphor is coated directly on the fiber-optic bundle; 0.43 mm corresponds to the case where the cone angle of the NA equals the cone angle of the solid angle that each of the 331 individual fibers subtends; and 3.18 mm corresponds to phosphor substrate thickness used in this study. An examination of the three cases for XUV beam size with radii less than 2 mm reveals that the most scintillated light is collected when the distance between the phosphor and the fiber optic bundle is 0.43 mm (C1/C2=7.5). According to the flux calculations, if the phosphor substrate thickness is reduced from 3.18 to 0.43 mm the sensitivity of C2 increases by a factor of 3. As shown in Fig. 6(a), decreasing the distance to 0.10 mm decreases the amount of light collected by the fiber-optic bundle; therefore, it is not advantageous to coat the phosphor directly on the fiber-optic bundle. In Fig. 6(b) the ratio of C1/C2 was evaluated with the NA of the fiber-optic bundle in C2 equal to 0.44 instead of 0.22. With the larger NA in Fig. 6(b) the optimal spacing between the phosphor and the fiber-optic bundle is 0.22 mm instead of 0.43 mm. A comparison of

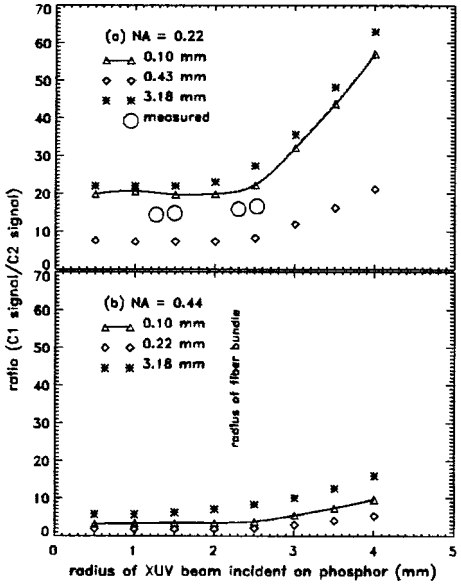

FIG. 6. Ratio of the estimated signals of detector configurations C1 and C2 as a function of the radius of the XUV beam incident on the P45 phosphor: (a) the ray tracing code used to estimate the measured signal in the C2 assumed a numerical aperture (NA) of 0.22 and the distance between the phosphor and the fiber was varied from 0.10 mm to 0.43 mm to 3.18 mm, (b) the same calculations were performed for C2 except the NA of 0.44 was assumed. Open circles represent measured results.

Figs. 6(a) and 6(b) reveals that if the spacing between the fiber and the phosphor is optimized, C2 will collect four times more scintillated visible light with the larger NA. The measured ratios (C1/C2) in Fig. 6(a) are represented by the open circles for the four incident beam sizes that were evaluated. The coupling of light in the cladding material, which was not considered in the ray tracing calculations, is likely to be the reason for the measured ratio being lower than the calculated ratio. The measured ratios of C1/C3 were evaluated for the four beam sizes presented in Fig. 6(a). The optical coupling of the visible scintillated light from the vacuum fiber to the atmosphere fiber at the fused fiber-optic faceplate introduced an additional loss of a factor of 6.7; therefore, the ratio of C1/C3 is about 100. Additional light loss experiments revealed that the fiber-optic faceplate used in C3 transmitted 48.5% of the visible scintillated light, and the atmosphere fiber-optic bundle used in C3 relayed 31.9% of the visible scintillated light from the faceplate to the PMT.

IV. DISCUSSION

The design and photometric calibration of a detector consisting of a P45 phosphor, two incoherent silica/silica fiber-optic bundles coupled with a vacuum feedthrough fiber-optic faceplate, and a PMT is reported. The silica/silica fiber was chosen in order to satisfy thermal and radiation hardness requirements of the tokamak environment.[12–14] Although the fiber-optic bundle provides the necessary flexibility required to position the spectroscopic diagnostic in close proximity to the tokamak plasma, the losses sustained by coupling the visible scintillated light from the phosphor to the PMT are substantial. The detector configuration C3 could be optimized by reducing the phosphor substrate thickness from 3.18 to 0.43 mm. This would reduce the ratio, C1/C3, from

100 to 33. In detector configuration C3, if the atmosphere incoherent fiber-optic bundle were eliminated and the PMT were mounted directly on the fused fiber-optic faceplate of the vacuum feedthrough, C1/C3 could be further reduced to 11. The effects of the electronic gain and photocathode material of the PMT on the photometric calibration were studied. The importance of matching the visible emission spectrum of the phosphor with photocathode of the PMT is evident in the higher CE of the P45/PMT combination with the bialkali photocathode. A systematic error was not evident in the comparison of our PMT electronic gain measurements with the gain measurements supplied with the tube from the manufacturer. Therefore, it is not clear whether the PMT gain measurement is dependent on the spectrum of the visible light source. However, this comparison of PMT electronic gain measurements points out the uncertainty in the absolute photometric calibration of a P45/PMT XUV photodetector associated with using the manufacturers measurement of the PMT electronic gain. Other ways to increase the overall conversion efficiency of the detector are to use higher intrinsic efficiency phosphors and to improve the collection efficiency of the visible scintillated photons. Rapid progress in generating artificially activated materials and understanding the processes involved in luminescence lead to the invention of phosphors that can be tailored for a particular application; however, high intrinsic luminescent efficiency and a fast time response appear to be mutually excluding properties of most phosphors.[15–17] The P45 phosphor has been chosen because its intrinsic efficiency of converting soft x-ray photons to the visible photons with the wavelength of about 5000 Å (green) is one of the highest.[18] The dependence of the phosphor intrinsic efficiency on its thickness, i.e., its physical reabsorption and scattering properties is not studied in this work, however, measurements and models developed recently[19] have been used to evaluate and optimize the phosphor layer. Other rare-earth phosphors which utilize additive dopant impurities for extrinsic luminescence are also used. Among others, the P46 ($Y_3Al_5O_{15}$:Ce) and P47 (Y_2SiO_5:Ce) phosphors have been shown to have adequate intrinsic efficiency and a time response of $\tau \simeq 0.1$ μs, much faster than the P45 time response of $\tau \leqslant 1$ ms.[19–22]

ACKNOWLEDGMENTS

The authors would like to acknowledge Dr. James Terry and Dr. Bruce Lipschultz of the Plasma Fusion Science Center at the Massachusetts Institute of Technology for supplying the fused fiber-optic faceplate used for these measurements. This research was performed at JHU under the auspices of U.S. DOE Grant No. DE-FG02-86ER53214.

[1] J. A. R. Samson, *Techniques of Vacuum Ultraviolet Spectroscopy* (Pied, Lincoln, NB, 1980).
[2] B. Zurro, C. Burgos, K. McCarthy, and L. Barquero, Rev. Sci. Instrum. **68**, 680 (1997).
[3] L. K. Huang, S. P. Regan, M. Finkenthal, and H. W. Moos, Rev. Sci. Instrum. **63**, 5171 (1992).
[4] S. P. Regan, M. Finkenthal, M. J. May, and H. W. Moos, Rev. Sci. Instrum. **66**, 770 (1995).
[5] M. J. May *et al.*, Rev. Sci. Instrum. **68**, 1047 (1997).
[6] V. A. Soukhanovskii *et al.*, Rev. Sci. Instrum. **70**, 340 (1999).
[7] V. A. Soukhanovskii *et al.*, Rev. Sci. Instrum. **72**, 3270 (2001).
[8] J. A. Goetz *et al.*, Plasma Phys. Controlled Fusion **6**, 1899 (1999).
[9] D. Stutman *et al.*, Rev. Sci. Instrum. **62**, 2719 (1991).
[10] S. P. Regan *et al.*, Appl. Opt. **33**, 3595 (1994).
[11] B. Henke *et al.*, At. Data Nucl. Data Tables **27**, 1 (1982).
[12] A. Ramsey, Rev. Sci. Instrum. **66**, 871 (1995).
[13] W. Tighe *et al.*, Rev. Sci. Instrum. **66**, 907 (1995).
[14] H. Adler, K. W. Hill, A. T. Ramsey, and W. Tighe, Rev. Sci. Instrum. **66**, 904 (1995).
[15] K. McCarthy *et al.*, J. Appl. Phys. **92**, 6541 (2002).
[16] S. J. Dhoble, J. Phys. D **33**, 158 (2000).
[17] S. E. Deranzo, M. J. Weber, E. Bourret-Courchesne, and M. K. Klintenberg, Nucl. Instrum. Methods Phys. Res. (in press).
[18] B. Zurro *et al.*, Rev. Sci. Instrum. **66**, 534 (1995).
[19] A. Baciero *et al.*, J. Appl. Phys. **85**, 6790 (1999).
[20] A. Baciero *et al.*, J. Synchrotron Radiat. **7**, 215 (2000).
[21] J. H. Chappell and S. S. Murray, Nucl. Instrum. Methods Phys. Res. A **221**, 159 (1984).
[22] B. X. Yang, J. Kirz, and S. Xu, Nucl. Instrum. Methods Phys. Res. A **258**, 141 (1984).